

The Primal versus the Dual Ising Model

Mehdi Molkaeraie

ETH Zurich

mehdi.molkaeraie@alumni.ethz.ch

Abstract—We represent the Ising model of statistical physics by normal factor graphs in the primal and in the dual domains. By analogy with Kirchhoff’s voltage and current laws, we show that in the primal normal factor graphs, the dependency among the variables is along the cycles, whereas in the dual normal factor graphs, the dependency is on the cutsets. In the primal (resp. dual) domain, dependent variables can be computed via their fundamental cycles (resp. fundamental cutsets). Using Onsager’s closed form solution, we illustrate the opposite behavior of the uniform sampling estimator for estimating the partition function in the primal and in the dual of the homogeneous Ising model on a two-dimensional torus.

I. INTRODUCTION

We relate some properties of the normal/Forney factor graph (NFG) [1] representation of the Ising model [2], [3] in the primal and in the dual domains to pertinent results in algebraic graph theory. The focus is on Ising models with arbitrary topology, with pairwise (nearest-neighbor) interactions, and without an external magnetic field.

Here, the NFG is a simple, finite, and connected graph $G = (V, E)$, where V is the set of vertices and E the set of edges. In our analysis, we use partitionings of G into $G = T \cup \bar{T}$, where T is a spanning tree and \bar{T} is the corresponding cospanning tree. The edges of T are called the *branches* and the edges of \bar{T} are called the *chords* of G with respect to T , or simply the chords of T . Since G is connected, $|E| \geq |V| - 1$ and

$$|T| = |V| - 1 \quad (1)$$

$$|\bar{T}| = |E| - |V| + 1, \quad (2)$$

where $|\cdot|$ denotes the cardinality of a set.

We prove that the sum (modulo 2) of variables along any cycle in the primal NFG is zero. In the dual NFG, we prove that the sum (modulo 2) of variables on any cutset is zero. We then propose a uniform sampling algorithm for estimating the partition function in the primal and in the dual domains. For the homogeneous Ising model on a two-dimensional (2D) torus, we employ Onsager’s analytical solution [3], [4] to illustrate the opposite behavior of the uniform sampling estimator in the primal and in the dual domains.

For more details on the cycle space, the cutset space, and their duality in the context of algebraic graph theory, see [5, Chapter 2], [6, Chapter 14]. The topic of the Kramers–Wannier duality (which relates the partition function of the 2D Ising model at high and at low temperatures) is discussed in the context of NFG duality in [7], [8]. Finally, we would like to point out that David Forney has recently developed

and generalized some of the results of this paper in the context of algebraic topology. For more details, see [9].

The paper is organized as follows. In Section II, we review the Ising model and its graphical model representation in terms of NFGs. In Sections III and IV, we describe the uniform sampling algorithm in the primal domain and derive its variance for the Ising model on a 2D torus. The dual NFG of the model is discussed in Section V, and an analogous estimator based on uniform sampling in the dual NFG is presented in Section VI. The variance of the estimator in the dual NFG is discussed in Section VII. The scale factor between the partition functions of the primal and the dual NFGs is derived in the Appendix.

II. THE ISING MODEL IN THE PRIMAL DOMAIN

Let $\mathbf{X} = (X_1, X_2, \dots, X_N)$ be a collection of N interacting discrete random variables taking values in a finite alphabet \mathcal{X} , which in this context is equal to the binary field \mathbb{F}_2 and let x_i represents a possible realization of X_i . The vectors $\mathbf{x} \in \mathcal{X}^N$ will be called configurations.

The variables X_1, X_2, \dots, X_N are associated with the vertices of a graph $G = (V, E)$ with N vertices and $|E|$ edges. In the Ising model, each variable is assigned a spin, which represents the two possible states of a particle. Two variables interact if their corresponding vertices are connected by an edge in G . Each edge has an associated coupling parameter $J_{k,\ell}$, which measures the strength of the interaction between neighboring pair (X_k, X_ℓ) .

Let $f: \mathcal{X}^N \rightarrow \mathbb{R}_{\geq 0}$ be a non-negative real function which factors into a product of local factors $v_{k,\ell}(\cdot)$ as

$$f(\mathbf{x}) = \prod_{(k,\ell) \in E} v_{k,\ell}(x_k, x_\ell), \quad (3)$$

where E contains all the unordered distinct interacting pairs (k, ℓ) , and $v_{k,\ell}: \mathcal{X}^2 \rightarrow \mathbb{R}_{\geq 0}$ is given by

$$v_{k,\ell}(x_k, x_\ell) = \begin{cases} e^{\beta J_{k,\ell}}, & \text{if } x_k = x_\ell \\ e^{-\beta J_{k,\ell}}, & \text{if } x_k \neq x_\ell, \end{cases} \quad (4)$$

where β is the inverse temperature. The Ising model is called ferromagnetic (resp. antiferromagnetic) if $J_{k,\ell} > 0$ (resp. $J_{k,\ell} < 0$) for all $(k, \ell) \in E$.

We will find it convenient to set $\beta = 1$ and to work with varying values of the coupling parameters. In this setup, large values of $|J_{k,\ell}|$ correspond to the low-temperature regime, and small values of $|J_{k,\ell}|$ correspond to the high-temperature regime. In particular, $J_{k,\ell} = 0$ for all $(k, \ell) \in E$ corresponds to infinite temperature.

From (3), the Boltzmann distribution is defined as [3]

$$p_B(\mathbf{x}) \triangleq \frac{f(\mathbf{x})}{Z}. \quad (5)$$

Here, Z is the *partition function*, which makes $p_B(\cdot)$ a probability mass function over \mathcal{X}^N , and is given by

$$Z = \sum_{\mathbf{x}} f(\mathbf{x}), \quad (6)$$

where the summation runs over all configurations.

The factorization in (3) can be represented by an NFG $G = (V, E)$, in which vertices represent the factors and edges represent the variables. The edge that represents some variable x is connected to the vertex representing the factor $v(\cdot)$ if and only if x is an argument of $v(\cdot)$. If a variable (an edge) appears in more than two factors, such a variable is replicated using an equality indicator factor [1].

The primal NFGs of the Ising model on a chain (1D graph with periodic boundaries), a 2D lattice, and a fully-connected graph are shown in Fig. 1, where the unlabeled boxes represent (4) and boxes labeled “=” are equality indicator factors. For example, in Fig. 1–left the equality indicator factor $\Phi_{=}(\cdot)$ involving variables x_2, x'_2 , and x''_2 is given by

$$\Phi_{=}(x_2, x'_2, x''_2) = \delta(x_2 - x'_2) \cdot \delta(x_2 - x''_2), \quad (7)$$

where $\delta(\cdot)$ is the Kronecker delta function.

We note that each factor (4) is only a function of $x_k + x_\ell$. (Recall that arithmetic manipulations are done modulo 2.) We can thus represent $v_{k,\ell}(\cdot)$ using only one variable y_e , as

$$v_e(y_e) = \begin{cases} e^{J_e}, & \text{if } y_e = 0 \\ e^{-J_e}, & \text{if } y_e = 1. \end{cases} \quad (8)$$

Let \mathbf{Y} denote $(Y_1, Y_2, \dots, Y_{|E|})$, where $|\mathbf{Y}| = |E|$.

Following the above observation, we construct the “modified” primal NFGs of the Ising models illustrated in Fig. 2, where the unlabeled boxes represent (8) and boxes labeled “+” are zero-sum indicator factors, which impose the constraint that all their incident variables sum to zero. For example, in Fig. 2–left the zero-sum indicator factor $\Phi_{+}(\cdot)$ involving x_1, x_2 , and y_1 is given by

$$\Phi_{+}(y_1, x_1, x_2) = \delta(y_1 + x_1 + x_2). \quad (9)$$

In the sequel, we drop the adjective “modified” and refer to the NFGs in Fig. 2 as the primal NFGs of the Ising model, when it causes no confusion.

By analogy with Kirchhoff’s voltage law, we prove:

Lemma 1. Consider a cycle in the primal NFG of the Ising model. If the variables attached to the zero-sum indicator factors along the cycle are Y_1, Y_2, \dots , it holds that

$$\sum_{m \in \text{Cycle}} Y_m = 0 \quad (10)$$

Proof. We write each Y_m as the addition of its corresponding edges (X_k, X_ℓ) attached to the zero-sum indicator factors along the cycle (see (9)). Each variable, say X_k , will appear twice in the summation. Thus $\sum_{m \in \text{Cycle}} Y_m = 0$. ■

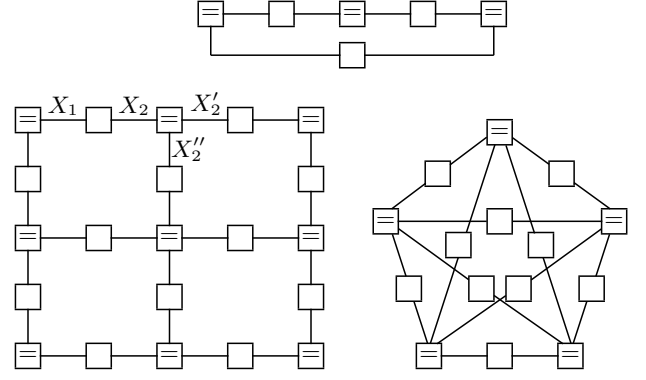


Fig. 1: The Primal NFG of the Ising model on a (top) chain (left) 2D lattice (right) fully-connected graph. The unlabeled boxes represent (4) and boxes containing “=” symbols are given by (7).

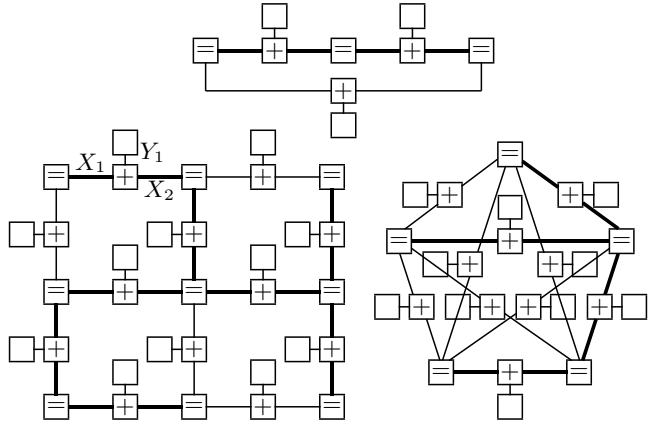


Fig. 2: Modified primal NFGs of the Ising models on a (top) chain (left) 2D lattice (right) fully-connected graph.. The unlabeled boxes represent (8), boxes containing “+” symbols are as in (9), and boxes containing “=” symbols are given by (7). In each NFG, the branches of a spanning tree are marked by thick black edges.

An example of a cycle is shown by thick edges in Fig. 3, where the variables Y_1, Y_2, \dots attached to the zero-sum indicator factors along the cycle are marked blue.

Let us partition G into $G = T \cup \bar{T}$, where T is a spanning tree in the primal NFG. Thus \mathbf{Y} will also be partitioned into $\mathbf{Y}_T \cup \mathbf{Y}_{\bar{T}}$. Examples of such partitionings are shown in Fig. 2, where spanning trees are marked by thick black edges, edges attached to the unlabeled boxes and to the zero-sum indicator factors on the branches represent \mathbf{Y}_T , and edges attached to the unlabeled boxes and to the zero-sum indicator factors on the chords represent $\mathbf{Y}_{\bar{T}}$.

For a given configuration \mathbf{y}_T , adding a chord $c \in \bar{T}$ to T will create a unique cycle called the fundamental cycle associated with c , which contains exactly one chord that does not appear in any other fundamental cycle¹. Furthermore,

¹Indeed, the set of all fundamental cycles generates a vector space over \mathbb{F}_2 with dimensionality $|\bar{T}|$; see [5, Chapter 2], [6, Chapter 14].

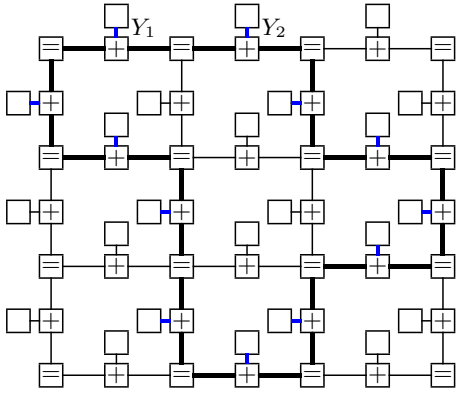


Fig. 3: Thick edges show a cycle in the primal NFG of the 2D Ising model, where variables attached to the zero-sum indicator factors along the cycle are marked blue.

according to Lemma 1, for each $c \in \bar{T}$ we can compute y_c as a linear combination of \mathbf{y}_T .

Remark 1. In the primal NFG, we can freely choose a configuration \mathbf{y}_T , and therefrom deterministically compute each component of $\mathbf{y}_{\bar{T}}$ via its fundamental cycle. As a result, computing the exact value of Z in the primal NFG requires a sum with $|\mathcal{X}|^{|\bar{T}|} = |\mathcal{X}|^{N-1}$ terms.

Accordingly, let

$$\Upsilon(\mathbf{y}) = \prod_{e \in E} v_e(y_e). \quad (11)$$

The global probability mass function in the modified primal NFG can then be defined as

$$p_M(\mathbf{y}) \triangleq \frac{\Upsilon(\mathbf{y})}{Z_M}, \quad (12)$$

where the partition function Z_M is given by

$$Z_M = \sum_{\text{valid } \mathbf{y}} \Upsilon(\mathbf{y}). \quad (13)$$

Lemma 2. The partition functions Z and Z_M are related by

$$Z = 2Z_M \quad (14)$$

Proof. Let $\neg \mathbf{x}$ be the component-wise addition of \mathbf{x} and the all-ones vector, i.e., in $\neg \mathbf{x}$, components of \mathbf{x} that are 0 become 1, and those that are 1 become 0. There are $|\mathcal{X}|^N$ configurations \mathbf{x} that contribute to Z in (6). Let us partition \mathcal{X}^N into \mathcal{X}_1 and \mathcal{X}_2 , where for each $\mathbf{x} \in \mathcal{X}_1$, we have $\neg \mathbf{x} \in \mathcal{X}_2$, and vice-versa. Note that $|\mathcal{X}_1| = |\mathcal{X}_2| = |\mathcal{X}|^{N-1}$.

There are $|\mathcal{X}|^{N-1}$ configurations \mathbf{y} with non-zero contributions to Z_M in (13). From one such configuration \mathbf{y} , we can compute exactly two corresponding configurations \mathbf{x} and $\neg \mathbf{x}$ in the primal NFG (e.g., by setting $x_1 = 0$ and $x_1 = 1$ to solve a system of equations for \mathbf{x} and for $\neg \mathbf{x}$). However, due to symmetry in the factors (4), the contribution of \mathbf{x} and of $\neg \mathbf{x}$ to Z is exactly $\Upsilon(\mathbf{y})$. ■

For 2D lattices, Lemmas 1 and 2 have already been observed in [10]. However, as was shown, their generalizations to models with arbitrary topology is straightforward.

Similar results can be obtained for the q -state Potts model, in which $v_{k,\ell}(\cdot)$ is only a function of $x_k - x_\ell$ (with arithmetic manipulations done modulo q). It can be shown that, for this model, $Z = qZ_M$ and dependency among the variables is along the cycles of a directed NFG.

We next propose a uniform sampling algorithm to compute an estimate of Z_M , and hence of Z itself.

III. UNIFORM SAMPLING IN THE PRIMAL NFG

In uniform sampling, we first draw independent samples $\mathbf{y}_T^{(1)}, \mathbf{y}_T^{(2)}, \dots$ uniformly over $\mathcal{X}^{|\bar{T}|}$, i.e., according to

$$u_T(\mathbf{y}_T) = \frac{1}{|\mathcal{X}^{|\bar{T}|}}, \quad (15)$$

and therefrom compute $\mathbf{y}_{\bar{T}}^{(1)}, \mathbf{y}_{\bar{T}}^{(2)}, \dots$. The created samples are then used in

$$\hat{Z}_M = \frac{|\mathcal{X}^{|\bar{T}|}}{L} \sum_{\ell=1}^L \Upsilon(\mathbf{y}^{(\ell)}), \quad (16)$$

which is an unbiased estimator of Z_M , i.e., $\mathbb{E}_{u_T}[\hat{Z}_M] = Z_M$.

The variance of (16) can be computed as

$$\mathbb{V}[\hat{Z}_M] = \mathbb{E}[\hat{Z}_M^2] - \mathbb{E}[\hat{Z}_M]^2, \quad (17)$$

$$= \frac{|\mathcal{X}^{2|\bar{T}|}}{L} \left(\sum_{\mathbf{y}} u_T(\mathbf{y}) \Upsilon(\mathbf{y})^2 \right) - \frac{Z_M^2}{L}, \quad (18)$$

$$= \frac{Z_M^2}{L} \left(\sum_{\mathbf{y}} \frac{p_M(\mathbf{y})^2}{u_T(\mathbf{y})} - 1 \right). \quad (19)$$

We thus obtain

$$\frac{L}{Z_M^2} \mathbb{V}[\hat{Z}_M] = \chi^2(p_M, u_T), \quad (20)$$

where $\chi^2(\cdot, \cdot)$ denotes the chi-square distance, which is non-negative, with equality to zero if and only if its two arguments are equal [11, Chapter 4].

Suppose the model is homogeneous (i.e., with constant coupling parameter J). In the limit $J \rightarrow 0$, $\Upsilon(\cdot)$ becomes a constant factor (cf. (8), (11)), therefore we expect the uniform sampling estimator to perform well when coupling parameters are small (i.e., at high temperature).

Indeed

$$\lim_{J \rightarrow 0} \chi^2(p_M, u_T) = 0. \quad (21)$$

IV. VARIANCE OF THE UNIFORM SAMPLING ALGORITHM IN THE PRIMAL 2D ISING MODEL

We analyze the variance of the uniform sampling estimator in the primal domain to estimate the partition function of the Ising model on a 2D torus, with constant coupling parameter J and in the thermodynamic limit (i.e., as $N \rightarrow \infty$). The choice of the model and the parameters is due to the fact that the partition function is analytically available from Onsager's solution in this case [4], [3, Chapter 7]. In a 2D torus, it holds that $|\bar{T}| = N - 1$ and $|\bar{T}| = N + 1$.

From (20), we have

$$\frac{L}{Z_M(J)^2} \mathbb{V}[\hat{Z}_M] = \sum_{\text{valid } \mathbf{y}} \frac{p_M(\mathbf{y})^2}{u_T(\mathbf{y})} - 1, \quad (22)$$

$$= \frac{|\mathcal{X}|^{|T|}}{Z_M(J)^2} \sum_{\text{valid } \mathbf{y}} \Upsilon(\mathbf{y})^2 - 1, \quad (23)$$

$$= |\mathcal{X}|^{N-1} \frac{Z_M(2J)}{Z_M(J)^2} - 1, \quad (24)$$

where $Z_M(J)$ denotes the partition function evaluated at J , and the last step is due to the following identity

$$Z_M(2J) = \sum_{\text{valid } \mathbf{y}} \Upsilon(\mathbf{y})^2. \quad (25)$$

Thus, in the thermodynamic limit we obtain

$$\begin{aligned} \lim_{N \rightarrow \infty} \frac{1}{N} \ln \left(1 + \frac{L}{Z_M(J)^2} \mathbb{V}[\hat{Z}_M] \right) &= \\ \ln(2) + \lim_{N \rightarrow \infty} \frac{\ln Z_M(2J)}{N} - \lim_{N \rightarrow \infty} \frac{2 \ln Z_M(J)}{N}. \end{aligned} \quad (26)$$

We use the closed-form solution of the partition function to evaluate (26) numerically as a function of J , which is plotted by the solid black line in Fig. 6. As expected, we observe that uniform sampling in the primal domain can provide good estimates of the partition function when J is small (i.e., at high temperature), while it is an inefficient estimator for larger values of J (i.e., at low temperature).

V. THE ISING MODEL IN THE DUAL DOMAIN

The dual NFG has the same topology as the primal NFG, but factors are replaced by the discrete Fourier transform (DFT) of their corresponding factors in the primal NFG, and variables are replaced by their corresponding dual variables, which are denoted by the tilde symbol. The partition function of the corresponding dual NFG is denoted by Z_d .

According to the normal factor graph duality theorem [12], $Z_d = \alpha(G) \cdot Z$, where the scale factor $\alpha(G)$ depends on the topology of G and is given by

$$\alpha(G) = |\mathcal{X}|^{|E|-|V|}. \quad (27)$$

The proof of (27) is given in the Appendix. For example, for a 2D torus $|E| = 2N$, and therefore $\alpha(G) = |\mathcal{X}|^N$; for a chain $|E| = |V|$, and thus $\alpha(G) = 1$.

Notice that from (2), (14), and (27), we obtain

$$Z_d/Z_M = \alpha(G)/|\mathcal{X}|, \quad (28)$$

$$= |\mathcal{X}|^{|\bar{T}|}. \quad (29)$$

From the primal NFG of an Ising model, we can obtain its dual by replacing each factor (8) by its 1D DFT, each equality indicator factor by a zero-sum indicator factor, and each zero-sum indicator factor by an equality indicator factor.

The dual NFGs of the Ising models in Fig. 2 are shown in Fig. 4, where the unlabeled boxes represent factors as

$$\gamma_e(\tilde{y}_e) = \begin{cases} 2 \cosh J_e, & \text{if } \tilde{y}_e = 0 \\ 2 \sinh J_e, & \text{if } \tilde{y}_e = 1, \end{cases} \quad (30)$$

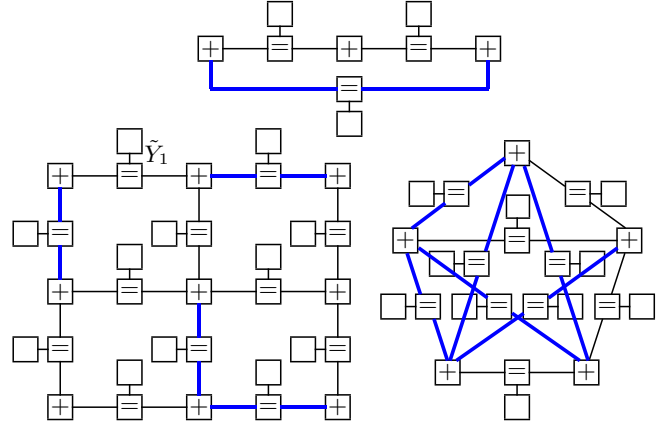


Fig. 4: Dual NFGs of the Ising models in Fig. 2. The unlabeled boxes represent (30), boxes containing “+” symbols are as in (9), and boxes containing “=” symbols are given by (7). In each dual NFG, the chords are marked by thick blue edges.

boxes labeled “+” are zero-sum indicator factors as in (9), and boxes containing “=” symbols are equality indicator factors given by (7). For more details on constructing the dual NFG of the Ising model, see [13]–[16].

By analogy with Kirchhoff’s current law, we prove:

Lemma 3. Consider a cutset in the dual NFG of the Ising model. If the variables attached to the equality indicator factors in the cutset are $\tilde{Y}_1, \tilde{Y}_2, \dots$, it holds that

$$\sum_{m \in \text{Cutset}} \tilde{Y}_m = 0 \quad (31)$$

Proof. A cutset partitions G into $G_1 \cup G_2$. In G_1 (or in G_2), suppose we write down the equations associated with all the zero-sum indicator factors. But the sum over all these equations in G_1 (or in G_2) is equal to zero, because each variable, say \tilde{Y}_k , appears twice in the summation. Furthermore, in G , the same sums are equal to $\sum_{m \in \text{Cutset}} \tilde{Y}_m$. ■

An example of a cutset is shown by thick edges in Fig. 5, where the variables $\tilde{Y}_1, \tilde{Y}_2, \dots$ attached to the equality indicator factors in the cutset are marked blue.

Again, we partition G into $G = T \cup \bar{T}$, where T is a spanning tree in the dual NFG. As a result, $\tilde{\mathbf{Y}} = \tilde{\mathbf{Y}}_T \cup \tilde{\mathbf{Y}}_{\bar{T}}$. Fig. 4 shows examples of such partitionings, where cospanning trees are marked by thick blue edges, edges attached to the unlabeled boxes and to the equality indicator factors on the branches represent $\tilde{\mathbf{Y}}_T$, and edges attached to the unlabeled boxes and to the equality indicator factors on the chords represent $\tilde{\mathbf{Y}}_{\bar{T}}$. Although T is always cycle-free, \bar{T} may contain cycles (see Fig. 4–right).

Removing a branch $b \in T$ partitions $T = T_1 \cup T_2$. The edges that connect T_1 and T_2 form a unique cutset in G – called the fundamental cutset belonging to b . Each fundamental cutset has exactly one branch of T that does

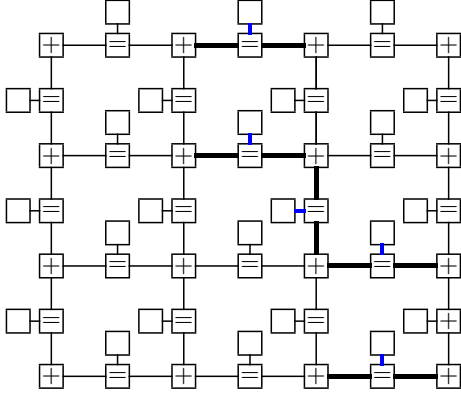


Fig. 5: Thick edges show a cutset in the dual NFG of the 2D Ising model, where variables on the cutset are marked blue.

not appear in any other fundamental cutset². Moreover, according to Lemma 3, for each $b \in T$ we can compute \tilde{y}_b as a linear combination of $\tilde{\mathbf{y}}_{\bar{T}}$.

Remark 2. In the dual NFG, we can freely choose a configuration $\tilde{\mathbf{y}}_{\bar{T}}$, and therefrom deterministically compute each component of $\tilde{\mathbf{y}}_T$ via its fundamental cutset. In the dual NFG, computing the exact value of Z_d (and thus the exact value of Z_M) requires a sum with $|\mathcal{X}|^{|\bar{T}|}$ terms. In particular, computing Z_d of a chain requires a sum with $|\mathcal{X}|$ terms.

Let

$$\Gamma(\tilde{\mathbf{y}}) = \prod_{e \in E} \gamma_e(\tilde{y}_e). \quad (32)$$

Suppose the model is “ferromagnetic” (i.e., $J_{k,\ell} > 0$ for all $(k, \ell) \in E$), thus $\Gamma(\cdot)$ is non-negative. We then define the following global probability mass function in the dual NFG

$$p_d(\tilde{\mathbf{y}}) \triangleq \frac{\Gamma(\tilde{\mathbf{y}})}{Z_d}, \quad (33)$$

where

$$Z_d = \sum_{\text{valid } \tilde{\mathbf{y}}} \Gamma(\tilde{\mathbf{y}}). \quad (34)$$

Next, we propose a uniform sampling algorithm in the dual NFG to estimate Z_d .

VI. UNIFORM SAMPLING IN THE DUAL NFG

In uniform sampling in the dual domain, samples $\mathbf{y}_{\bar{T}}^{(1)}, \mathbf{y}_{\bar{T}}^{(2)}, \dots$ are drawn independently according to

$$u_{\bar{T}}(\tilde{\mathbf{y}}_{\bar{T}}) = \frac{1}{|\mathcal{X}|^{|\bar{T}|}}, \quad (35)$$

and completed to valid configurations $\mathbf{y}^{(1)}, \mathbf{y}^{(2)}, \dots$. Then L created samples are used in the following estimator

$$\hat{Z}_d = \frac{|\mathcal{X}|^{|\bar{T}|}}{L} \sum_{\ell=1}^L \Gamma(\tilde{\mathbf{y}}^{(\ell)}), \quad (36)$$

²In the dual domain, the set of all fundamental cutsets generates a vector space over \mathbb{F}_2 with dimensionality $|T|$; see [5, Chapter 2], [6, Chapter 14].

which is unbiased, that is, $\mathbb{E}_{u_{\bar{T}}}[\hat{Z}_d] = Z_d$ (see [16]).

The variance of (36) is given by

$$\frac{L}{Z_d^2} \mathbb{V}[\hat{Z}_d] = \chi^2(p_d, u_{\bar{T}}). \quad (37)$$

In the low temperature limit p_d becomes uniform over the valid configurations (cf. (30), (32)). The estimator is thus expected to perform well in the low-temperature regime (i.e., for large J). Indeed

$$\lim_{J \rightarrow \infty} \chi^2(p_d, u_{\bar{T}}) = 0. \quad (38)$$

VII. VARIANCE OF THE UNIFORM SAMPLING ALGORITHM IN THE DUAL 2D ISING MODEL

In the dual domain, we provide upper and lower bounds on the variance of the estimator. The derived bounds are not necessarily tight for all values of J ; however, they are good enough to illustrate the opposite behavior of (16) and (36).

From (37), we have

$$\frac{L}{Z_d(J)^2} \mathbb{V}[\hat{Z}_d] = \sum_{\text{valid } \tilde{\mathbf{y}}} \frac{p_d(\tilde{\mathbf{y}})^2}{u_{\bar{T}}(\tilde{\mathbf{y}})} - 1, \quad (39)$$

$$= \frac{|\mathcal{X}|^{|\bar{T}|}}{Z_d(J)^2} \sum_{\text{valid } \tilde{\mathbf{y}}} \Gamma(\tilde{\mathbf{y}})^2 - 1, \quad (40)$$

$$= \frac{2^{N+1}}{Z_d(J)^2} S_d - 1, \quad (41)$$

where $S_d \triangleq \sum_{\text{valid } \tilde{\mathbf{y}}} \Gamma(\tilde{\mathbf{y}})^2$.

From (27) and (14), we obtain $Z_d = 2^{N+1} Z_M$, therefore

$$\frac{L}{Z_d(J)^2} \mathbb{V}[\hat{Z}_d^{\text{Uni}}] = \frac{2^{-N-1}}{Z_M(J)^2} S_d - 1. \quad (42)$$

In the rest of this section, we will derive upper and lower bounds on S_d . We first apply the obvious inequality

$$S_d \leq Z_d(J)^2 \quad (43)$$

in (41) to obtain

$$\lim_{N \rightarrow \infty} \frac{1}{N} \ln \left(1 + \frac{L}{Z_d(J)^2} \mathbb{V}[\hat{Z}_d^{\text{Uni}}] \right) \leq \ln(2), \quad (44)$$

which is plotted by the solid blue line in Fig. 6.

We next note that S_d is the partition function of a dual NFG (as in Fig. 4–left) with factors given by

$$\rho(\tilde{y}_e) = \begin{cases} 4 \cosh(J)^2, & \text{if } \tilde{y}_e = 0 \\ 4 \sinh(J)^2, & \text{if } \tilde{y}_e = 1. \end{cases} \quad (45)$$

Thus

$$S_d = \sum_{\text{valid } \tilde{\mathbf{y}}} \prod_{e \in E} \rho(\tilde{y}_e), \quad (46)$$

$$\leq (4 \cosh(J)^2)^{|\bar{T}|} \sum_{\tilde{\mathbf{y}}_{\bar{T}} \in \bar{T}} \prod_{e \in \bar{T}} \rho(\tilde{y}_e), \quad (47)$$

$$= (2 \cosh(J))^{2(N-1)} S_{\bar{T}}. \quad (48)$$

Here, $S_{\bar{T}}$ is the partition function of a subgraph in the dual NFG induced by \bar{T} , which can be computed exactly as

$$S_{\bar{T}} = (\rho(0) + \rho(1))^{|\bar{T}|}, \quad (49)$$

$$= (4 \cosh(2J))^{N+1}. \quad (50)$$

Combining (42), (48), and (50) yields

$$\lim_{N \rightarrow \infty} \frac{1}{N} \ln \left(1 + \frac{L}{Z_d(J)^2} \mathbb{V}[\hat{Z}_d] \right) \leq 3 \ln(2) + \ln \left(\cosh(2J) \cdot \cosh(J)^2 \right) - \lim_{N \rightarrow \infty} \frac{2 \ln Z_M(J)}{N}, \quad (51)$$

which is plotted by the dotted blue line in Fig. 6.

To obtain the lower bound, we consider the corresponding primal NFG (as in Fig. 2–left) with factors as in

$$\kappa(y_e) = \begin{cases} 2 \cosh(2J), & \text{if } y_e = 0 \\ 2, & \text{if } y_e = 1. \end{cases} \quad (52)$$

Notice that (52) is indeed the inverse Fourier transform of (45). We denote the partition function of this primal NFG by S_M , where according to the NFG duality theorem

$$S_d = 2^{N+1} S_M, \quad (53)$$

see (29). Hence

$$S_M = \sum_{\text{valid } \mathbf{y}} \prod_{e \in E} \kappa(y_e), \quad (54)$$

$$\geq 2^{|T|} \sum_{\mathbf{y}_T} \prod_{e \in T} \kappa(y_e), \quad (55)$$

$$= 2^{N+1} S_T, \quad (56)$$

where S_T denotes the partition function of a subgraph in the primal NFG induced by T (i.e., a spanning tree), which again can be computed exactly as

$$S_T = (\kappa(0) + \kappa(1))^{|T|}, \quad (57)$$

$$= (2 \cosh(J))^{2N-2}, \quad (58)$$

see [3, Chapter 2], [13, Section III].

From (53), (56), and (58) we obtain

$$S_d \geq 2^{4N} \cosh(J)^{2(N-1)}. \quad (59)$$

Combining (42) and (59) gives the following lower bound

$$\lim_{N \rightarrow \infty} \frac{1}{N} \ln \left(1 + \frac{L}{Z_d(J)^2} \mathbb{V}[\hat{Z}_d] \right) \geq 3 \ln 2 + 2 \ln \left(\cosh(J) \right) - \lim_{N \rightarrow \infty} \frac{2 \ln Z_M(J)}{N}, \quad (60)$$

which is shown by the dashed red line in Fig. 6.

From Fig. 6, we observe that uniform sampling in the dual domain is inefficient for small values of J ; however, compared to uniform sampling in the primal domain, it can provide more reliable estimates of the partition function when J is large. Alos, recall from Section VI that (37) vanishes in the low-temperature limit (i.e., as $J \rightarrow \infty$).

Both estimators seem to be inefficient in the mid-temperature regime and near *criticality*, which for this model is located at $J_c = \frac{1}{2} \ln(1 + \sqrt{2}) \approx 0.44$ (see [3, Chapter 6]).

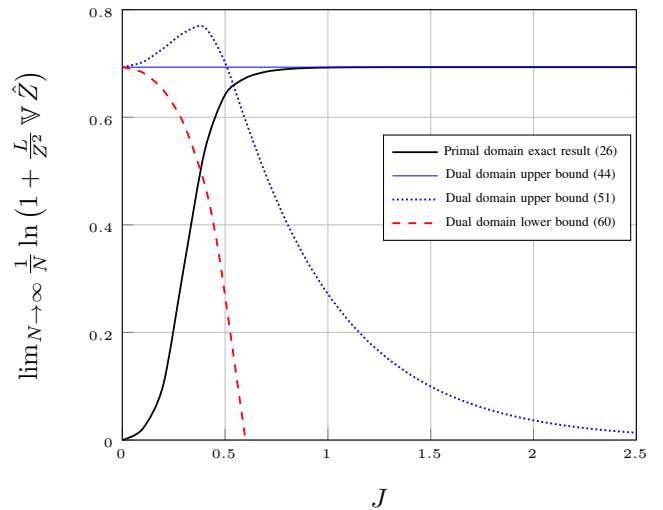


Fig. 6: Behavior of the variance of the uniform sampling estimator in the primal and in the dual NFGs as a function of the coupling parameter J , for a homogeneous 2D Ising model in the thermodynamic limit. The solid black line shows (26), the solid blue line shows the upper bound in (44), the dotted blue line shows the upper bound in (51), and the dashed red line shows the lower bound in (60).

VIII. CONCLUSION

We analyzed some properties of the Ising model (in the primal and in the dual domains) in the context of algebraic graph theory. We showed that, in the primal domain, variables can be freely chosen on a spanning tree, and the remaining variables can be computed via their fundamental cycles, whereas in the dual domain, we can choose the variables arbitrarily on a cospanning tree, and compute the remaining variables via their fundamental cutsets. In each domain, a uniform sampling algorithm was proposed to estimate the partition function, and its opposite behavior was illustrated for the homogeneous Ising model on a 2D torus.

APPENDIX

DETAILS OF THE SCALE FACTOR

For completeness, we prove that the scale factor between the partition function Z of an NFG and the partition function Z_d of the corresponding dual NFG is

$$\alpha(G) = |\mathcal{X}|^{|E|-|V|}, \quad (61)$$

where $\alpha(G) = Z_d/Z$, which depends on the topology of G .

We will use the following concepts: a box is a collection of factors as illustrated by the dashed lines in Fig. 7, and the *exterior function* of such a box is the product of all factors inside the box, summed over all variables inside the box [12]. For example, the exterior function of the inner dashed box in Fig. 7 is given by

$$g(x_1, x_3, x_5) = \sum_{x_2} f_1(x_1, x_2, x_5) f_2(x_2, x_3), \quad (62)$$

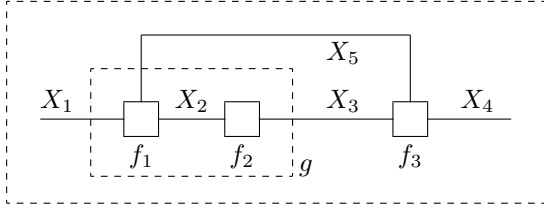


Fig. 7: Boxes in an NFG.

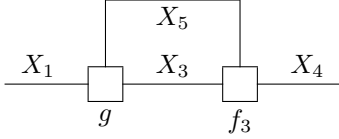


Fig. 8: Closing the inner box in Fig. 7.

and the exterior function of the outer dashed box in Fig. 7 is given by

$$Z = \sum_{x_1, \dots, x_5} f_1(x_1, x_2, x_5) f_2(x_2, x_3) f_3(x_3, x_4, x_5). \quad (63)$$

Closing a box means replacing it by a single factor that represents the exterior function of the box. Thus, closing the inner box in Fig. 7 yields the NFG in Fig. 8. Opening a box means the reverse process of expanding a factor into an NFG of its own (with the same exterior function).

Remark. closing a box (by summing over the internal variables) and opening a box do not change the partition function.

For ease of exposition, we consider NFGs with pairwise interactions between the variables (but with arbitrary topology). We demonstrate the dualization procedure by its application to the NFG shown in Fig. 9, which shows an edge of the NFG with factor $f_{k,\ell}(\cdot)$ connected to two equality indicator factors. To obtain the dual NFG, the dualization procedure needs to be applied throughout the primal NFG.

The procedure consists of three steps. In the first step, we insert an equality indicator factor into every edge, as shown in Fig. 10. More precisely, we split each edge, say X_ℓ , into two edges X_ℓ and X'_ℓ , which we reconnect via an equality indicator factor. Clearly, the partition function remains unchanged (since configurations in which $X_\ell \neq X'_\ell$ do not contribute to the partition function).

In the second step, we expand each of the newly inserted equality indicator factors into the product of a (scaled) Fourier kernel \mathcal{F} and a (scaled) inverse Fourier kernel \mathcal{F}^* , as depicted in Fig. 11. We assume that all variables take on values in a finite set \mathcal{X} . Indeed

$$\mathcal{F}(x_\ell, \tilde{x}_\ell) = e^{-i2\pi x_\ell \tilde{x}_\ell / |\mathcal{X}|}, \quad (64)$$

and

$$\mathcal{F}^*(x'_\ell, \tilde{x}_\ell) = e^{i2\pi x'_\ell \tilde{x}_\ell / |\mathcal{X}|}, \quad (65)$$

where i is the unit imaginary number [17].

The exterior function of the right dashed box in Fig. 11 is

$$\sum_{\tilde{x}_\ell} c_\ell \mathcal{F}(x_\ell, \tilde{x}_\ell) c'_\ell \mathcal{F}^*(x'_\ell, \tilde{x}_\ell) = c_\ell c'_\ell |\mathcal{X}| \cdot \delta(x_\ell - x'_\ell) \quad (66)$$

and so forth.

An obvious choice for the constants c and c' is such that

$$c_\ell c'_\ell |\mathcal{X}| = 1. \quad (67)$$

In the third step, we regroup the factors as illustrated in Fig. 12. Closing the dashed boxes in Fig. 12 yields the dual NFG in Fig. 13, where the factor $f_{k,\ell}(\cdot)$ is replaced by its Fourier transform $\tilde{f}_{k,\ell}(\cdot)$, and the equality indicator factors $\Phi_=(\cdot)$ are replaced by their inverse Fourier transforms, which are zero-sum indicator factors $\Phi_+(\cdot)$ – up to scale.

As in the rest of this paper, we choose the scale factors c_ℓ and c'_ℓ as

$$c_\ell = c'_\ell = \frac{1}{|\mathcal{X}|^{1/2}}. \quad (68)$$

With this choice, the Fourier transform of (4) is indeed equal to (30), and the inverse Fourier transform of an equality indicator factor with degree d is

$$\frac{1}{|\mathcal{X}|^{d/2}} \sum_{x'_{\ell_1}, \dots, x'_{\ell_d}} \Phi_=(x'_{\ell_1}, \dots, x'_{\ell_d}) \prod_{i=1}^d \mathcal{F}^*(x'_{\ell_i}, \tilde{x}_{\ell_i}), \quad (69)$$

which is easily verified to be

$$|\mathcal{X}|^{1-d/2} \cdot \Phi_+(\tilde{x}_{\ell_1}, \dots, \tilde{x}_{\ell_d}). \quad (70)$$

The (global) scale factor $\alpha(G)$ can then be computed by multiplying all the local scale factors as

$$\alpha(G) = \prod_{i=1}^N |\mathcal{X}|^{\frac{d_i}{2} - 1}, \quad (71)$$

$$= |\mathcal{X}|^{\frac{1}{2} \sum_{i=1}^N d_i - |V|}, \quad (72)$$

$$= |\mathcal{X}|^{|E| - |V|}, \quad (73)$$

where d_i denotes the degree of the i -th equality indicator factor, $|V|$ is the number of vertices (which is equal to N), and $|E|$ denotes the number of edges.

It should be emphasized that i) the scale factors c_ℓ and c'_ℓ (which were introduced in the second step) can be chosen differently, with a corresponding effect on $\alpha(G)$, and ii) the sequence of \mathcal{F} and \mathcal{F}^* on every edge is arbitrary; but the choice will affect the resulting dual NFG.

ACKNOWLEDGEMENTS

The author would like to thank Hans-Andrea Loeliger for his help and advice in providing the Appendix. The author also wishes to thank David Forney, Pascal Vontobel, Christoph Pfister, Justin Dauwels, Stefan Moser, and Vicenç Gómez for their comments on an earlier version of this paper.

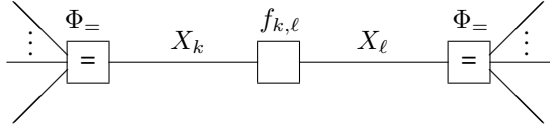


Fig. 9: An edge of an NFG with pairwise interactions used to demonstrate the dualization procedure. The factor $f_{k,\ell}(\cdot)$ is connected to two equality indicator factors.

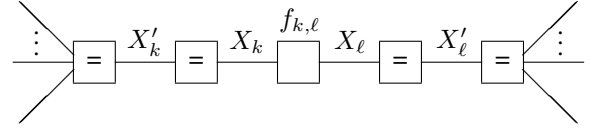


Fig. 10: Inserting an equality indicator factor on every edge of the NFG in Fig. 9. The partition function remains unchanged.

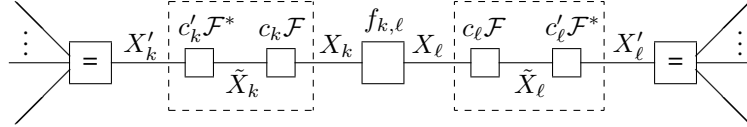


Fig. 11: Factoring each equality indicator factor in Fig. 10 into a Fourier transform and an inverse Fourier transform.

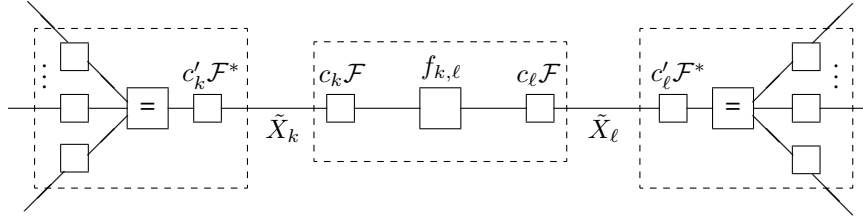


Fig. 12: Regrouping the factors in Fig. 11 and closing the dashed boxes yields the dual NFG.

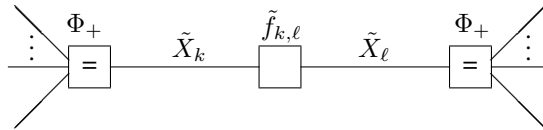


Fig. 13: The corresponding edge in the dual of the NFG in Fig. 9.

REFERENCES

- [1] G. D. Forney, Jr., "Codes on graphs: normal realization," *IEEE Trans. on Information Theory*, vol. 47, pp. 520–548, Feb. 2001.
- [2] B. A. Cipra, "An introduction to the Ising model," *American Math. Monthly*, vol. 94, pp. 937–959, Dec. 1987.
- [3] R. J. Baxter, *Exactly Solved Models in Statistical Mechanics*. Dover Publications, 2007.
- [4] L. Onsager, "Crystal statistics. I. A two-dimensional model with an order-disorder transition," *Phys. Rev.*, vol. 65, pp. 117–149, Feb. 1944.
- [5] B. Bollobás, *Modern Graph Theory*. Springer, 1998.
- [6] C. Godsil and G. Royle, *Algebraic Graph Theory*. Springer, 2001.
- [7] A. Al-Bashabsheh and P. Vontobel, "The Ising model: Kramers-Wannier duality and normal factor graphs," *Proc. 2015 IEEE Int. Symp. on Information Theory*, Hong Kong, June 14–19, 2015, pp. 2266–2270.
- [8] A. Al-Bashabsheh and P. Vontobel, "A factor-graph approach to algebraic topology, with applications to Kramers-Wannier duality," [arXiv:1607.02361](https://arxiv.org/abs/1607.02361), 2017.
- [9] G. D. Forney, Jr., "Graphical models for elementary algebraic topology, with applications to statistical physics and codes on graphs," [arXiv:1707.06621](https://arxiv.org/abs/1707.06621), 2017.
- [10] F. Y. Wu and Y. K. Wang, "Duality transformation in a many-component spin model," *Journal of Math. Phys.*, vol. 17, pp. 439–440, March 1976.
- [11] I. Csiszár and P. C. Shields, *Information Theory and Statistics: A Tutorial*. Foundations and Trends in Communications and Information Theory, vol. 1, pp. 417–528, Dec. 2004.
- [12] A. Al-Bashabsheh and Y. Mao, "Normal factor graphs and holographic transformations," *IEEE Trans. on Information Theory*, vol. 57, pp. 752–763, Feb. 2011.
- [13] M. Molkaiaie and H.-A. Loeliger, "Partition function of the Ising model via factor graph duality," *Proc. 2013 IEEE Int. Symp. on Information Theory*, Istanbul, Turkey, July 7–12, 2013, pp. 2304–2308.
- [14] A. Al-Bashabsheh and Y. Mao, "On stochastic estimation of the partition function," *Proc. 2014 IEEE Int. Symp. on Information Theory*, Honolulu, USA, June 29–July 4, 2014, pp. 1504–1508.
- [15] M. Molkaiaie, "An importance sampling scheme for models in a strong external field," *Proc. 2015 IEEE Int. Symp. on Information Theory*, Hong Kong, June 14–19, 2015, pp. 1179–1183.
- [16] M. Molkaiaie, "An importance sampling algorithm for the Ising model with strong couplings," *Proc. 2016 Int. Zurich Seminar on Communications*, March 2–4, 2016, pp. 180–184.
- [17] D. W. Kammler, *A First Course in Fourier Analysis*. Cambridge University Press, 2007.